



## RESEARCH LETTER

10.1029/2023GL103699

## A Lagrangian Estimate of the Mediterranean Outflow's Origin

G. Vecchioni<sup>1</sup> , P. Cessi<sup>2</sup> , N. Pinardi<sup>1,3</sup> , Louise Rousselet<sup>2,4</sup>, and F. Trotta<sup>3</sup>

### Key Points:

- Eighty-six percent of Mediterranean outflow originates from the Gulf of Lions, and 13% originates from the Strait of Sicily
- These two components of the outflow have distinct T-S distributions at the origin, but the distinction is lost when Gibraltar is reached
- Median transit times to the Strait of Gibraltar are 5 years from the Gulf of Lions and 8 years from the Strait of Sicily

### Supporting Information:

Supporting Information may be found in the online version of this article.

### Correspondence to:

P. Cessi,  
pcessi@ucsd.edu

### Citation:

Vecchioni, G., Cessi, P., Pinardi, N., Rousselet, L., & Trotta, F. (2023). A Lagrangian estimate of the Mediterranean outflow's origin. *Geophysical Research Letters*, 50, e2023GL103699. <https://doi.org/10.1029/2023GL103699>

Received 14 MAR 2023  
Accepted 13 JUN 2023

### Author Contributions:

**Conceptualization:** P. Cessi, N. Pinardi  
**Data curation:** F. Trotta  
**Formal analysis:** G. Vecchioni  
**Funding acquisition:** P. Cessi, N. Pinardi  
**Methodology:** G. Vecchioni, P. Cessi, N. Pinardi, Louise Rousselet  
**Software:** G. Vecchioni, Louise Rousselet, F. Trotta  
**Supervision:** P. Cessi, N. Pinardi  
**Validation:** G. Vecchioni  
**Visualization:** G. Vecchioni  
**Writing – original draft:** P. Cessi  
**Writing – review & editing:** G. Vecchioni, N. Pinardi, Louise Rousselet

© 2023. The Authors.

This is an open access article under the terms of the [Creative Commons Attribution-NonCommercial-NoDerivs License](https://creativecommons.org/licenses/by/4.0/), which permits use and distribution in any medium, provided the original work is properly cited, the use is non-commercial and no modifications or adaptations are made.

<sup>1</sup>Department of Physics and Astronomy, University of Bologna, Bologna, Italy, <sup>2</sup>Scripps Institution of Oceanography, University of California, San Diego, La Jolla, CA, USA, <sup>3</sup>Fondazione Centro EuroMediterraneo sui Cambiamenti Climatici, Bologna, Italy, <sup>4</sup>Laboratoire d'Océanographie et du Climat: Expérimentations et Approches Numériques (LOCEAN-IPSL, CNRS), Paris, France

**Abstract** The origin of the Mediterranean Outflow is investigated by deploying six millions virtual Lagrangian parcels at the Strait of Gibraltar, and tracing them backward in time using velocity estimates from an eddy-permitting reanalysis. The Lagrangian parcels are followed until they intercept one of three sections. The hypothesis is that each section is associated with distinct water masses: the Gulf of Lions, related to Western Mediterranean Deep Water and Western Intermediate Water, carries 86% of the Outflow's transport; the Northern Tyrrhenian, related to Tyrrhenian Deep and Intermediate Waters, carries 1% of the transport; the Strait of Sicily, related to Levantine Intermediate Waters, carries 13% of the transport. The median transit times from the sections to the Strait of Gibraltar range from 5 years (Gulf of Lions) to 8 years (Strait of Sicily).

**Plain Language Summary** Parcel trajectories are used to trace water masses from the Western Mediterranean Sea to the Mediterranean Sea outflow at the Strait of Gibraltar. The velocity advecting the parcels is an estimate combining observations with an ocean circulation model that conserves mass, momentum, temperature and salinity. It is found that 86% of the parcels in the Mediterranean Sea outflow originate from the Gulf of Lions, typically taking 5 years for the journey, while 13% originates from the Strait of Sicily, typically taking 8 years to complete the trip.

## 1. Introduction

The Mediterranean Sea is characterized by an anti-estuarine circulation where light water enters from the Atlantic, and intermediate and deep waters are formed, primarily because of the net negative buoyancy flux to the atmosphere (Schoeder & Chiggiato, 2023). The wind-stress and buoyancy-flux power an open overturning circulation entering at the Strait of Gibraltar as Atlantic Water (AW) in the upper layer and exiting at the Strait of Gibraltar as Mediterranean Outflow composed of denser waters formed within the Mediterranean Sea (Cessi et al., 2014; Pinardi et al., 2019).

The early paper of Bryden and Stommel (1982) laid the foundations for the study of the Mediterranean Outflow origin in terms of dense water mass sources in the Mediterranean Sea. Bryden and Stommel (1982) envisioned connecting the outflow to the Western Mediterranean Deep Waters (WMDW), formed in the Gulf of Lions, advocating the fundamental role of mixing and upwelling in the region of the anticyclonic Western Alboran Gyre. New data sets, collected in the Strait of Gibraltar, partially confirm this picture, implicating intermediate water masses as additional contributions to the outflow (García-Lafuente et al., 2017; Millot, 2014). Specifically, Millot (2014) and Naranjo et al. (2015) estimate the contribution of four water masses to the Mediterranean outflow from in situ data: WMDW, Western Intermediate Water (WIW), Tyrrhenian Deep Water (TDW) and Levantine Intermediate Water (LIW). WMDW and WIW are formed in the Liguro-Provençal gyre and northern shelf areas (Pinardi et al., 2023), hereafter called the Gulf of Lions. TDW originates in the Northern Tyrrhenian Sea, but this area is also responsible for intermediate water formation, called Tyrrhenian Intermediate Water (TIW) (Napolitano et al., 2019; Pinardi et al., 2023). LIW is formed in the easternmost part of the Mediterranean Sea basin and enters the Western Mediterranean from the Strait of Sicily.

The deep water formed in the Eastern basin (Roether et al., 1996; Schlitzer et al., 1991) is considered to be only a small fraction of the dense waters entering the western basin at the Strait of Sicily (Astraldi et al., 1999).

We focus on all three regions in the Western Mediterranean that contribute to the deep and intermediate waters composition of the Mediterranean Outflow: the Gulf of Lions, the Tyrrhenian Sea and the Strait of Sicily.



A classical approach to differentiating water masses is to assume linear mixing on a T-S diagram, attributing specific point in the T-S plane to each water mass. García-Lafuente et al. (2021) apply this method to their measurements at the Espartel sill, that is, on the Atlantic side of the Strait of Gibraltar, using LIW, WMDW, and AW as the water-mass types composing the Mediterranean Outflow. They find approximately 75% WMDW and 25% LIW in the years 2005–2014.

In the following we offer a complementary approach to estimating the fractional composition of the Mediterranean Outflow: we trace the origin of the Mediterranean Outflow using virtual Lagrangian parcels advected backwards in time from the Strait of Gibraltar by the three-dimensional eddy-permitting velocity provided by a Mediterranean Sea reanalysis. In addition to quantitatively determining the volume of LIW, WMDW/WIW and TDW/TIW composing the Mediterranean outflow, we demonstrate that the histograms of parcel occurrence in T-S space at each origin section—the Gulf of Lions, the Strait of Sicily, and the Northern Tyrrhenian Sea—exhibit broad distributions, peaked at the expected water-mass types. In addition, the Lagrangian analysis provides transit-time distributions for each pathway.

## 2. Lagrangian Analysis and Reanalysis

Virtual parcel trajectories and their T-S properties are obtained using the velocity and tracers fields of the eddy-permitting Mediterranean Sea reanalysis (Simoncelli et al., 2014). The data set consists of daily mean outputs of zonal and meridional velocities, temperature and salinity fields from 1987 to 2018, defined on the model native grid (Mesinger & Arakawa, 1976). The subset of data spanning years 2000–2012 is used because it includes the decade of the circulation adjusted with satellite altimetry and Argo. Additionally, this decade partially overlaps with the analysis of García-Lafuente et al. (2021).

The ocean model used by the reanalysis is NEMO (Madec et al., 2022) which solves the primitive equations with a spherical coordinate system. The grid has a horizontal resolution of  $1/16^\circ \times 1/16^\circ$  and 72 unevenly spaced vertical layers. The model is nested in the Atlantic within the monthly mean climatological fields of a global model. Air-sea fluxes of momentum, heat and water are computed with bulk formulas based on the ERA-Interim reanalysis fields from the European Centre for Medium-Range Weather Forecasts (ECMWF).

The temperature and salinity profiles from CTDs, XBTs, MBTs, bottles and Argo floats, provided by different European databases, together with along-track satellite altimetry sea-level anomalies, are assimilated by a three-dimensional variational system (Dobricic & Pinardi, 2008). Satellite sea surface temperature (SST) is used to correct the model heat flux at the air-sea interface by a relaxation of the surface temperature toward the observed SST.

The quality of the Mediterranean reanalysis has been assessed in Simoncelli et al. (2014). This reanalysis has been used to map the mean circulation of the Mediterranean Sea (Pinardi et al., 2015) and it has allowed the investigation of the residual overturning circulation (Pinardi et al., 2019).

To track the origin of the water masses associated with the Mediterranean outflow, virtual parcels are seeded in the Mediterranean side of the Strait of Gibraltar, at  $5.25^\circ\text{W}$ , and then advected backwards in time for 78 years, allowing 99.8% to reach one of the control sections. This requires looping the data set, which covers 13 years, six times. The discontinuities in the velocity and tracer fields associated with looping can introduce errors, which are significantly reduced by using a large set of parcels (Döös et al., 2017; Thomas et al., 2015). A large number of parcels is required to obtain accurate quantitative diagnostics, as suggested by Döös (1995). Parcels are released at the Strait of Gibraltar every day from 1 January 2005 to 31 December 2012, during the first cycle of the loop (8 years). The sum of all parcels initialized over these 8 years is about 6 million. The initialization period (2005–2012) is shorter than the looping period (2000–2012) to allow backward advection for at least 5 years by the proximal velocities, before looping is introduced.

Three-dimensional Lagrangian trajectories are computed using the parcel-tracking software “Ariane,” developed by Blanke and Raynaud (1997). Since the reanalysis does not store vertical velocity, this field is computed from the horizontal velocity fields using the incompressibility condition, with the same discretization of the reanalysis' numerical model. Each parcel is tagged with a small volume transport whose maximum is  $10^{-3}$  Sv. Because the velocity field is non-divergent, the volume transport initially assigned to each parcel is conserved along the trajectory. Conservation of volume allows to evaluate the transport contribution from each origin-section to the

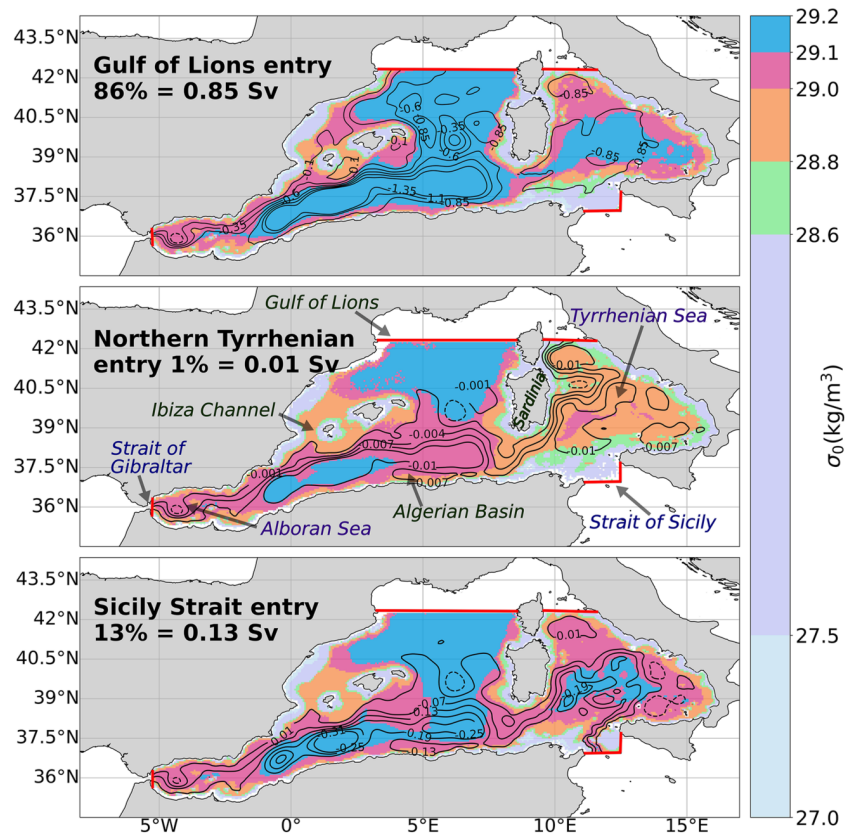


**Figure 1.** Lagrangian streamlines quantifying volume transport pathways from each of the three entry sections to the exit section, all shown as red lines. Solid (dashed) black contours represent negative (positive) values. Streamfunction contour intervals are: 0.25 Sv for the Gulf of Lions entry (contours with absolute values larger than 1.35 Sv are omitted—the minimum value is  $-4.55$  Sv); 0.003 Sv for the Northern Tyrrhenian entry (contours with absolute values larger than 0.01 Sv are omitted—the minimum value is  $-0.03$  Sv); 0.06 Sv for the Strait of Sicily entry (contours with absolute values larger than 0.31 Sv are omitted—the minimum value is  $-0.56$  Sv). The color shading shows  $\langle \sigma \rangle$  (defined in Supporting Information S1). The Strait of Gibraltar (exit section) is located at  $5.25^\circ\text{W}$  with latitudes from  $35.69^\circ\text{N}$  to  $36.31^\circ\text{N}$ . The Gulf of Lions and Northern Tyrrhenian sections are located at the same latitude ( $42.31^\circ\text{N}$ ), in the longitude ranges  $3.31^\circ\text{E}$ – $8.63^\circ\text{E}$  for the first and  $9.5^\circ\text{E}$ – $11.56^\circ\text{E}$  for the second. The section at the Strait of Sicily has two segments: one spans  $11.13^\circ\text{E}$ – $12.5^\circ\text{E}$ , at  $36.94^\circ\text{N}$ ; the other is at  $12.5^\circ\text{E}$  spanning latitudes  $36.94^\circ\text{N}$ – $37.63^\circ\text{N}$ .

Strait of Gibraltar. The number of parcels seeded daily on a grid cell at the initial section is proportional to the daily transport crossing that cell (Blanke & Raynaud, 1997). Because parcels within a grid cell have different initial positions, their trajectories diverge exponentially in a few days (d’Ovidio et al., 2004; García-Olivares et al., 2007). No Lagrangian diffusion is implemented in the calculation of trajectories. More details of the Lagrangian technique are in Supporting Information S1.

When parcels are advected backward in time, the origin of each parcel is defined as the first section intercepted among those depicted in the middle panel of Figure 1, during the 78 years of integration. The “first passage” identifies the “entry” section, while the Strait of Gibraltar is the “exit” section, common to all parcels as the seeding location. The locations of the entry and exit sections are given in the caption of Figure 1.

The estimated outflow transport, obtained from the cumulative transport of all the seeded parcels averaged over the 2005–2012 period, is  $-1.13$  Sv. Parcels that first exit the entry section at Gibraltar are considered to be inflow of Atlantic origin and their transport, amounting to 0.14 Sv, is removed from the outflow transport. Thus, the Lagrangian-average Mediterranean outflow is  $-0.99$  Sv. Parcels that do not reach any section in 78 years are considered lost and discarded from the calculation: these amount to 0.0019 Sv. Finally, the parcels that intercept the surface and evaporate (0.0001 Sv) are also excluded in the estimate of the outflow transport. We note that the Lagrangian-average of the outflow,  $-0.99$  Sv, is larger than the time-averaged Eulerian estimate for the same

period, which amounts to  $-0.92$  Sv. The Lagrangian ensemble-average represents the residual circulation rather than the time-averaged Eulerian flow (Rousselet et al., 2020), and their difference is due to rectified wave/eddy flow (Flierl, 1981). The residual and Eulerian zonal overturning circulations in the Mediterranean have been shown to differ, with the deep residual cell exceeding its Eulerian counterpart (Pinardi et al., 2019).

### 3. Routes of the Mediterranean Outflow

Following the technique proposed by Blanke et al. (1999), the major pathways are displayed by the Lagrangian streamfunction of the vertically integrated transport, obtained by summing all the parcels transport recorded at each velocity grid point. The Lagrangian streamlines thus obtained represent the ensemble average of parcel trajectories. Even though every parcel path is open and connects the entry and exit sections, closed streamlines exist. They are a signature of trajectories spiraling in three dimensions that appear closed in this two-dimensional average. Henceforth, results are presented and discussed forward in time.

The Lagrangian estimate of the average outflow from the Mediterranean Sea to the Atlantic at the Strait of Gibraltar over the period 2005–2012 is larger than the Eulerian time averaged for the same data set and larger than that obtained by Sammartino et al. (2015) with a high resolution hindcast model informed by current meter observations of a vertical profile at the Espartel Sill. It is also larger than recent observational estimates, based on the same profile measurements extrapolated over a whole section of the Strait of Gibraltar, which gives an outflow value of  $0.85 \pm 0.13$  Sv (García-Lafuente et al., 2021). Given the differences between Lagrangian and Eulerian estimates, we emphasize the percentage rather than the absolute value of the transport in the partition among different routes.

According to our Lagrangian analysis, the majority of this outflow, 86% (0.85 Sv) originates from the Gulf of Lions entry section, while 13% (0.13 Sv) originates from the Strait of Sicily entry section, and 1% (0.01 Sv) from the Northern Tyrrhenian entry section. The partition between the Gulf of Lions and Strait of Sicily Lagrangian origins is consistent with the observational estimate of García-Lafuente et al. (2021) for the period 2005–2014 based on water-type analysis. Because at  $5.25^\circ\text{W}$  the Strait of Gibraltar extends down to  $\sim 800$  m, it is reasonable that the percentage of Gulf-of-Lions water at our section is larger than the estimates of García-Lafuente et al. (2021), which are based on observations of WMDW collected at the shallower Espartel Sill ( $\sim 350$  m). Furthermore, the Gulf-of-Lions transport includes contributions of LIW and WIW, augmenting the fraction originating at this section.

The Lagrangian transport streamlines, computed with the subset of parcels from each entry section to the exit section, are shown in Figure 1 (black contours), superimposed on a map of the associated ensemble-average potential density,  $\langle \sigma \rangle$  (color shading), defined in Supporting Information S1. The top panel of Figure 1 displays the Gulf of Lions route. Most of the transport exits the Gulf of Lions on the western side, following the Northern Current (Millot, 1990). Further along, the majority turns south-eastward around the Balearic islands, and is associated with the spreading of WMDW, with  $\sigma_0 > 29.1$ . Before exiting the Mediterranean Sea, WMDW spirals cyclonically in the Algerian Basin, slowly upwelling from about 1,600 to 800 m (closed streamlines with absolute values larger than 0.85 Sv). The Lagrangian streamlines in this region are consistent with the observed trajectories of profiling floats drifting between 2,000 and 1,200 m analyzed by Testor et al. (2005).

In an additional pathway, WMDW flows through the Sardinia channel and then spirals in the Tyrrhenian Sea (contour  $-0.85$  Sv). This pathway confirms the potential role of WMDW in the formation of TDW. Finally, the streamline  $-0.1$  Sv, crossing the Ibiza Channel with  $\sigma_0 < 29.1$ , identifies WIW, flowing directly to the Strait of Gibraltar. Thus, our analysis confirms that WIW is a component of the Mediterranean Outflow as described by Millot (2014).

The middle panel of Figure 1 shows the streamfunction associated with the pathway connecting the Northern Tyrrhenian entry to the Gibraltar Strait outflow. Here parcels follow the Bonifacio dipole, a cyclonic-anticyclonic pair arranged north-south with the Bonifacio Cyclone (Anticyclone) to the north (south), as observed in Napolitano et al. (2019). The cyclonic recirculation within the Tyrrhenian Sea is essentially along the isopycnal with  $29 > \sigma_0 > 28.8 \text{ kg/m}^3$ . After flowing through the Sardinia Channel, parcels spiral cyclonically in the Algerian Basin, at depths between 600 and 1,200 m, that is, shallower than the Gulf of Lions route.

The main density transformations of the parcels originating in the Gulf of Lions and Tyrrhenian occur in the Alboran Sea, especially around the Western Alboran Gyre: here parcels with density above  $\sigma_0 > 29.1$  ascend to

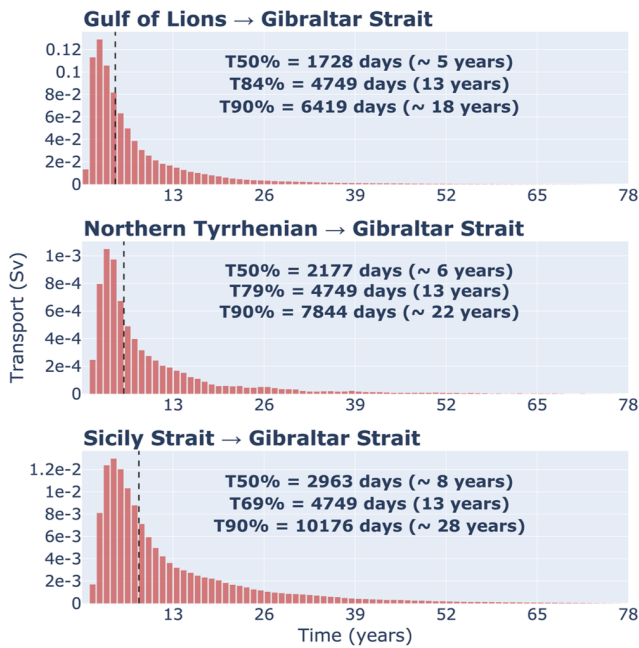


**Figure 2.** Transport-weighted transit time distribution between each entry section and the exit section, as specified at the top of each panel. Each bin corresponds approximately to 1 year. Dashed line indicates the transport-weighted median time, T50%, displayed on the side along with the 90th percentile, T90%, and the percentage of transits under 13 years.

shallower depths. Changes in  $\sigma_0$  along the streamlines are especially prominent near the southern boundary of the Western Alboran Gyre, suggesting that this region is the main mixing and upwelling site for dense water masses that have to climb the Gibraltar sill to exit the Mediterranean Sea.

The bottom panel of Figure 1 shows the streamfunction associated with the pathway connecting the Strait of Sicily to the Gibraltar Strait outflow. After leaving the Strait of Sicily, LIW parcels turn north-eastward in the deep Tyrrhenian basin. They circulate cyclonically in the Tyrrhenian Sea, reaching their highest densities,  $\sigma_0 > 29.1$ , and depths (about 1,250 m) before exiting through the Sardinia channel. The most significant pathway ( $-0.1$  Sv) exits the Sardinia channel, and recirculates around the gyres of the Algerian Basin.

The pathway of LIW in the Algerian Basin toward the Strait of Gibraltar has been amply discussed in the literature. Some authors (Puillat et al., 2006) indicate that the flow of LIW is primarily effected by anticyclonic eddies which divert LIW northward and westward. Our analysis shows an anticyclonic eddy-like feature around  $6.5^\circ\text{E}$  and  $39.5^\circ\text{N}$  with a small recirculation ( $0.05$  Sv) that occupies depths around 1,250 m.

The bulk of the transport exiting the Sardinia channel spirals in the Algerian Basin, showing three cyclonic recirculations (indicated by contours with absolute values larger than  $0.2$  Sv), similar to the cyclonic sub-gyres observed by Testor et al. (2005). Within these recirculations, LIW becomes denser, residing at depths of about 1,250 m. The Western Alboran Gyre induces an anticyclonic recirculation, steering most of the transport along the Moroccan Shelf and slope, while decreasing the density and depth of the water mass, which is a common feature of all three pathways composing the outflow.

In all three panels of Figure 1 large density gradients are found in the region between the Algerian Basin and the Western Alboran Gyre: here the ensemble averaged  $\sigma_0$  changes between 28.8 and 29.2 over small distances along the streamlines, a hallmark of diabatic changes.

The distributions of transport-weighted transit times for all three routes are shown in Figure 2. The fastest group arrives from the Gulf of Lions, with a median time of about 5 years, while the slowest group is from the Strait of Sicily, with median transit times of about 8 years. The group from the Strait of Sicily, which is representative of the LIW path, has transit times consistent with the analysis of Mallil et al. (2022) ( $\sim 3.3$  years of transit in the Algerian basin), and comparable to the transit times of LIW from its formation region to the Strait of Sicily (Roether et al., 1998). Notice that the Strait-of-Sicily group covers a larger distance than the group from the Gulf of Lions, and all of it recirculates within the Tyrrhenian Sea.

The Northern Tyrrhenian Sea group, which is the least populated, has a median transit time of about 6 years, intermediate between the other two. Notice that the Strait of Sicily section is approximately at the same distance from the Strait of Gibraltar as the Northern Tyrrhenian Sea section, but its transit times are longer. This is because the parcels from the Strait of Sicily are denser, following deeper routes both within the Tyrrhenian Sea and within the Western Mediterranean, and are thus advected by velocities that are generally weaker.

The first 13 years of advection, before any velocity-looping starts, captures 84% (Gulf of Lions), 79% (Tyrrhenian Sea) and 69% (Strait of Sicily) of the parcels trajectories, respectively, reassuring that the statistics presented are marginally affected by looping.

#### 4. Thermohaline Properties of Water Masses According to Routes

The binned transport-weighted T-S histograms in Figure 3 show the thermohaline properties for parcels at each entry section (left) and exit section (right).

The left panels of Figure 3 show that the thermohaline properties are clearly distinct for each entry section. Waters from the Eastern Mediterranean (Strait of Sicily entry—bottom panel) are clearly identified by the highest

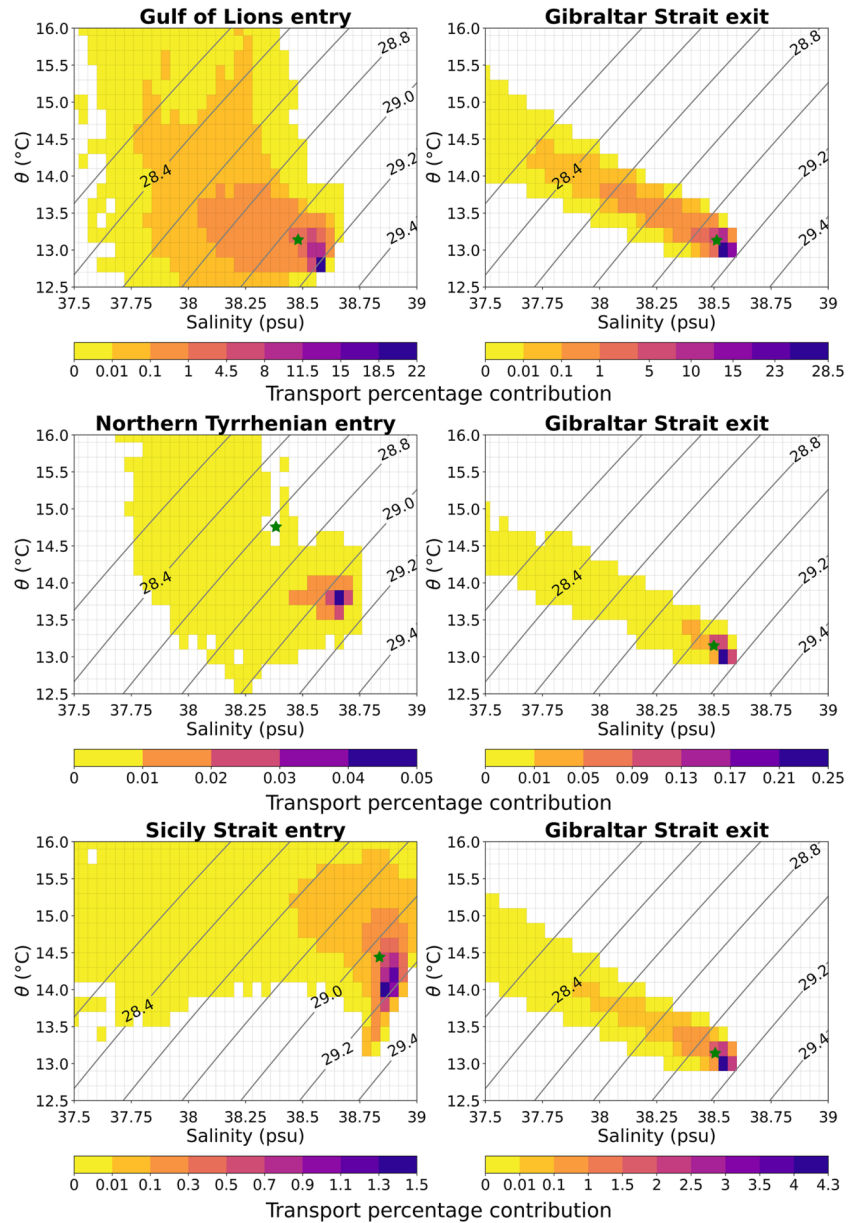


**Figure 3.** Potential temperature and salinity characteristics of the different water masses contributions to the 2005–2012 mean outflow at the each entry section (left) and at the exit section (right). Thermohaline properties are represented by summing the percentage transport contributions of each parcel per 0.2°C and 0.04 psu bin (color shading). Note the different value range of the colorbars to best fit the different transport associated with each entry section. Gray contours represent potential isopycnals. The transport-weighted mean T-S values of each distribution are denoted by green stars.

salinity, reaching the value of 38.96 psu, and the highest temperatures (around 14°C), values that are characteristic of LIW. Comparing the bottom two panels, we observe that LIW parcels (i.e., the mode of the distribution) undergo most changes in temperature and salinity from entry to exit, but these changes are largely compensated in potential density space. The parcels identified by this group do not represent all the outflow from the Strait of Sicily into the Western Mediterranean, but just that portion that arrives at the Strait of Gibraltar before crossing any of the other entry sections in the Western Mediterranean Sea. Thus, the LIW pathways that contribute to TIW/TDW and WMDW formation at the other two entry sections are not considered.

The coldest and densest water comes from the Gulf of Lions (top left panel), where formation of WMDW takes place, whose characteristics dominate the core (i.e., the mode) of the distribution.

covers a wide range of higher temperatures and lower salinities, corresponding to WIW and near surface waters. For this group, the changes in temperature and salinity from entry to exit are limited, and are accompanied by comparable density changes, suggesting that small mixing processes are at work during the spreading of WMDW.

The core of the distributions at the Gulf of Lions and Strait of Sicily entries, and at the Strait of Gibraltar exit all lie on the same range of potential densities ( $29.1 < \sigma_0 < 29.2$ ), requiring mostly epipycnal mixing, with little diapycnal changes.

Finally, the small group from the Northern Tyrrhenian entry, with characteristics typical of both TIW and TDW undergoes the largest changes in T, S and potential density of all three groups.

The T-S diagrams show that the thermohaline characteristics at the exit section in the Strait of Gibraltar are very similar among all three groups, with the core of the distribution at 38.55 psu and 13.0°C for all three groups. The T-S diagrams in Figure 3 (right panels) agree quantitatively with direct observations at a nearby section (Naranjo et al., 2015, Figure 6b). In this sense, the contribution of LIW, WMDW and TIW is identifiable in each of our exit T-S diagrams. However, stirring and mixing, acting on the pathways common to the three groups (Tyrrhenian Sea, Algerian Basin, and Alboran Gyres), unify the T-S distributions at the Strait of Gibraltar, regardless of their distant origin. The Alboran Gyres, especially the southern flank of the Western Alboran Gyre, have been implicated before as the primary site of localized mixing processes that ultimately produce Mediterranean Outflow characteristics (Bryden & Stommel, 1982; García-Lafuente et al., 2017). WMDW and LIW, as well as TDW and TIW have been recognized in the Tyrrhenian Sea and Algerian Basin (Millot, 2009).

## 5. Conclusions

The origin of the Mediterranean Outflow in terms of the dense waters formed inside the Mediterranean Sea has been quantified with Lagrangian analysis. The velocity field of the eddy-permitting Mediterranean Sea reanalysis (Simoncelli et al., 2014) has been employed to advect virtual parcels, seeded at the Strait of Gibraltar, backward in time. We focused on a relatively recent period, 2000 to 2012, which assimilates satellite altimetry and Argo looping the velocity field six times, for a total of 78 years of backward advection.

Recent studies have indicated that different dense water masses compose the Mediterranean Outflow: WIW and WMDW from the Gulf of Lions region; TIW and TDW from the Northern Tyrrhenian Sea and LIW from the Strait of Sicily. The “first passage” concept, which amounts to a race to the Strait of Gibraltar exit from one of the three target entry sections, precludes estimating the contribution of TIW, TDW and LIW to WIW and WMDW. A different design of Lagrangian analysis is necessary to quantify these interactions.

The bulk of the outflow, 86%, comes from the Gulf of Lions, while 13% originates from the Strait of Sicily and 1% originates from the Northern Tyrrhenian Sea. The routes of the Mediterranean dense waters all recirculate in the Algerian Basin and in the deep Tyrrhenian basin, increasing the transit time of the waters and modifying their T-S characteristics.

The Lagrangian analysis provides distributions of transit times from the target entry sections to the Strait of Gibraltar, with median times ranging from 5 years (for the Gulf of Lions section) to 8 years (for the Strait of Sicily section). These transit times are consistent with estimates of segments of flows made by Mallil et al. (2022).

The cores of the probability density distributions of parcel occupation in T-S space at the entry sections identify the water mass properties that contribute to the Mediterranean Sea Outflow. Each entry section displays a broad range of T-S properties with large tails around the core of the distribution (the mode), and means that can differ substantially from the modes. The cores of the Gulf of Lions and Strait of Sicily entries both have potential densities very close to the core at the Strait of Gibraltar, but different T and S, requiring minimal net diapycnal mixing but substantial epipycnal changes.

As originally postulated by Bryden and Stommel (1982) and later supported by García-Lafuente et al. (2017) our analysis implicates the southern flank of Western Alboran Gyre as a site of localized mixing processes that ultimately produce the Mediterranean Outflow characteristics. We conjecture that additional stirring and mixing occurs along the portions of trajectories common to all groups, that is, the Tyrrhenian Sea and the Algerian basin.

Further experiments covering different time periods are required to investigate the interdecadal variability of the Mediterranean outflow. In particular, Lagrangian analysis could be applied to assess whether the warming

and acidification trends observed from 2013 onwards are induced by a larger fraction of LIW over WMDW, as suggested by the analysis of García-Lafuente et al. (2021). Additionally, we plan to use different seeding sections in both the Western and Eastern Mediterranean Sea to quantify the pathways within the whole basin.

## Data Availability Statement

The reanalysis data are available at [https://doi.org/10.25423/MEDSEA\\_REANALYSIS\\_PHYS\\_006\\_004](https://doi.org/10.25423/MEDSEA_REANALYSIS_PHYS_006_004). The Lagrangian software employed, Ariane version 2.3.0, is available at <http://ariane.lagrangian.free.fr/ariane.htm>. For reproducibility of all major results of the Lagrangian analyses performed for this study, the customized code of the Ariane software, the simulated Lagrangian trajectories, and post-processing scripts are made available through <https://github.com/giuli9/Ariane-postprocessing> and <https://doi.org/10.5281/zenodo.7705093>.

## References

- Astraldi, M., Balopoulos, S., Candela, J., Font, J., Gacic, M., Gasparini, G., et al. (1999). The role of straits and channels in understanding the characteristics of Mediterranean circulation. *Progress in Oceanography*, 44(1–3), 65–108. [https://doi.org/10.1016/s0079-6611\(99\)00021-x](https://doi.org/10.1016/s0079-6611(99)00021-x)
- Blanke, B., Arhan, M., Madec, G., & Roche, S. (1999). Warm water paths in the equatorial Atlantic as diagnosed with a general circulation model. *Journal of Physical Oceanography*, 29(11), 2753–2768. [https://doi.org/10.1175/1520-0485\(1999\)029<2753:WWPITE>2.0.CO;2](https://doi.org/10.1175/1520-0485(1999)029<2753:WWPITE>2.0.CO;2)
- Blanke, B., & Raynaud, S. (1997). Kinematics of the Pacific equatorial undercurrent: An Eulerian and Lagrangian approach from GCM results. *Journal of Physical Oceanography*, 27(6), 1038–1053. [https://doi.org/10.1175/1520-0485\(1997\)027<1038:KOTPEU>2.0.CO;2](https://doi.org/10.1175/1520-0485(1997)027<1038:KOTPEU>2.0.CO;2)
- Bryden, H. L., & Stommel, H. (1982). Origin of the Mediterranean outflow. *Journal of Marine Research*, 40, 55–71.
- Cessi, P., Pinardi, N., & Lyubartsev, V. (2014). Energetics of semienclosed basins with two-layer flows at the strait. *Journal of Physical Oceanography*, 44(3), 967–979. <https://doi.org/10.1175/JPO-D-13-0129.1>
- Dobricic, S., & Pinardi, N. (2008). An oceanographic three-dimensional variational data assimilation scheme. *Ocean Modelling*, 22(3–4), 89–105. <https://doi.org/10.1016/j.ocemod.2008.01.004>
- Döös, K. (1995). Inter-ocean exchange of water masses. *Journal of Geophysical Research*, 100(C7), 13499–13514. <https://doi.org/10.1029/95JC00337>
- Döös, K., Jönsson, B., & Kjellsson, J. (2017). Evaluation of oceanic and atmospheric trajectory schemes in the TRACMASS trajectory model v6.0. *Geoscientific Model Development*, 10(4), 1733–1749. <https://doi.org/10.5194/gmd-10-1733-2017>
- d’Ovidio, F., Fernández, V., Hernández-García, E., & López, C. (2004). Mixing structures in the Mediterranean Sea from finite-size Lyapunov exponents. *Geophysical Research Letters*, 31(17), L17203. <https://doi.org/10.1029/2004GL020328>
- Flierl, G. R. (1981). Particle motions in large-amplitude wave fields. *Geophysical & Astrophysical Fluid Dynamics*, 18(1–2), 39–74. <https://doi.org/10.1080/03091928108208773>
- García-Lafuente, J., Naranjo, C., Sammartino, S., Sánchez-Garrido, J. C., & Delgado, J. (2017). The Mediterranean outflow in the Strait of Gibraltar and its connection with upstream conditions in the Alborán Sea. *Ocean Science*, 13(2), 195–207. <https://doi.org/10.5194/os-13-195-2017>
- García-Lafuente, J., Sammartino, S., Huertas, I. E., Flecha, S., Sánchez-Leal, R. F., Naranjo, C., et al. (2021). Hotter and weaker Mediterranean outflow as a response to basin-wide alterations. *Frontiers in Marine Science*, 8. <https://doi.org/10.3389/fmars.2021.613444>
- García-Olivares, A., Isern-Fontanet, J., & García-Ladona, E. (2007). Dispersion of passive tracers and finite-scale Lyapunov exponents in the Western Mediterranean Sea. *Deep Sea Research Part I: Oceanographic Research Papers*, 54(2), 253–268. <https://doi.org/10.1016/j.dsr.2006.10.009>
- Madec, G., Bourdallé-Badie, R., Bouttier, P. A., Bricaud, C., Bruciaferri, D., Calvert, D., et al. (2022). *NEMO ocean engine*. Zenodo. <https://doi.org/10.5281/zenodo.6334656>
- Mallil, K., Testor, P., Bosse, A., Margirier, F., Houpert, L., Le Goff, H., et al. (2022). The Levantine intermediate water in the western Mediterranean and its interactions with the Algerian Gyres: Insights from 60 years of observation. *Ocean Science*, 18(4), 937–952. <https://doi.org/10.5194/os-18-937-2022>
- Mesinger, F., & Arakawa, A. (1976). *Numerical methods used in atmospheric models* (Vol. 1). GARP Publications Series.
- Millot, C. (1990). The Gulf of Lions’ hydrodynamics. *Continental Shelf Research*, 10(9–11), 885–894. [https://doi.org/10.1016/0278-4343\(90\)90065-5](https://doi.org/10.1016/0278-4343(90)90065-5)
- Millot, C. (2009). Another description of the Mediterranean Sea outflow. *Progress in Oceanography*, 82(2), 101–124. <https://doi.org/10.1016/j.pocean.2009.04.016>
- Millot, C. (2014). Heterogeneities of in-and out-flows in the Mediterranean Sea. *Progress in Oceanography*, 120, 254–278. <https://doi.org/10.1016/j.pocean.2013.09.007>
- Napolitano, E., Iacono, R., Ciuffardi, T., Reseghetti, F., Poulain, P.-M., & Notarstefano, G. (2019). The Tyrrhenian Intermediate Water (TIW) Characterization and formation mechanisms. *Progress in Oceanography*, 170, 53–68. <https://doi.org/10.1016/j.pocean.2018.10.017>
- Naranjo, C., Sammartino, S., García-Lafuente, J., Bellanco, M. J., & Taupier-Letage, I. (2015). Mediterranean waters along and across the Strait of Gibraltar, characterization and zonal modification. *Deep Sea Research Part I: Oceanographic Research Papers*, 105, 41–52. <https://doi.org/10.1016/j.dsr.2015.08.003>
- Pinardi, N., Cessi, P., Borile, F., & Wolfe, C. L. P. (2019). The Mediterranean Sea overturning circulation. *Journal of Physical Oceanography*, 49(7), 1699–1721. <https://doi.org/10.1175/JPO-D-18-0254.1>
- Pinardi, N., Estournel, C., Cessi, P., Escudier, R., & Lyubartsev, V. (2023). Chapter 7—Dense and deep water formation processes and Mediterranean overturning circulation. In K. Schroeder, & J. Chiggiato (Eds.), *Oceanography of the Mediterranean Sea* (pp. 209–261). Elsevier.
- Pinardi, N., Zavatarelli, M., Adani, M., Coppini, G., Fratianni, C., Oddo, P., et al. (2015). Mediterranean Sea large-scale low-frequency oceanographic variability and water mass formation rates from 1987 to 2007: A retrospective analysis. *Progress in Oceanography*, 132, 318–332. (Oceanography of the Arctic and North Atlantic Basins). <https://doi.org/10.1016/j.pocean.2013.11.003>
- Puillat, I., Sorgente, R., Ribotti, A., Natale, S., & Echevin, V. (2006). Westward branching of LIW induced by Algerian anticyclonic eddies close to the Sardinian slope. *Chemistry and Ecology*, 22(sup1), S293–S305. <https://doi.org/10.1080/02757540600670760>
- Roether, W., Klein, B., Beitzel, V., & Manca, B. B. (1998). Property distributions and transient-tracer ages in Levantine intermediate water in the eastern Mediterranean. *Journal of Marine Systems*, 18(1–3), 71–87. [https://doi.org/10.1016/S0924-7963\(98\)00006-2](https://doi.org/10.1016/S0924-7963(98)00006-2)

- Roether, W., Manca, B. B., Klein, B., Bregant, D., Georgopoulos, D., Beitzel, V., et al. (1996). Recent changes in eastern Mediterranean deep waters. *Science*, 271(5247), 333–335. <https://doi.org/10.1126/science.271.5247.333>
- Rousselet, L., Cessi, P., & Forget, G. (2020). Routes of the upper branch of the Atlantic meridional overturning circulation according to an ocean state estimate. *Geophysical Research Letters*, 47(18), e2020GL089137. <https://doi.org/10.1029/2020gl089137>
- Sammartino, S., García Lafuente, J., Naranjo, C., Sánchez Garrido, J. C., Sánchez Leal, R., & Sánchez Román, A. (2015). Ten years of marine current measurements in Espartel Sill, Strait of Gibraltar. *Journal of Geophysical Research: Oceans*, 120(9), 6309–6328. <https://doi.org/10.1002/2014JC010674>
- Schlitzer, R., Roether, W., Oster, H., Junghans, H.-G., Hausmann, M., Johannsen, H., & Michelato, A. (1991). Chlorofluoromethane and oxygen in the eastern Mediterranean. *Deep Sea Research Part I: Oceanographic Research Papers*, 38(12), 1531–1551. [https://doi.org/10.1016/0198-0149\(91\)90088-W](https://doi.org/10.1016/0198-0149(91)90088-W)
- Schoeder, K., & Chiggiato, J. (Eds.) (2023). *Mediterranean Sea oceanography*. Elsevier.
- Simoncelli, S., Fratianni, C., Pinardi, N., Grandi, A., Drudi, M., Oddo, P., & Srdjan, D. (2014). *Mediterranean Sea physical reanalysis (MEDREA)*. Copernicus Monitoring Environment Marine Service (CMEMS). [https://doi.org/10.25423/MEDSEA\\_REANALYSIS\\_PHYS\\_006\\_004](https://doi.org/10.25423/MEDSEA_REANALYSIS_PHYS_006_004)
- Testor, P., Send, U., Gascard, J.-C., Millot, C., Taupier-Letage, I., & Béranger, K. (2005). The mean circulation of the southwestern Mediterranean Sea: Algerian Gyres. *Journal of Geophysical Research*, 110(C11), C11017. <https://doi.org/10.1029/2004JC002861>
- Thomas, M. D., Tréguier, A.-M., Blanke, B., Deshayes, J., & Voldoire, A. (2015). A Lagrangian method to isolate the impacts of mixed layer subduction on the meridional overturning circulation in a numerical model. *Journal of Climate*, 28(19), 7503–7517. <https://doi.org/10.1175/JCLI-D-14-00631.1>